

# Analysis and simulation for the double corrugated cardboard plates under bending and in-plane shear force by homogenization method

Pham Tuong Minh DUONG

**Abstract**—In this paper, an analytic homogenization model under bending and in-plane shear force for the double corrugated cardboard plates is presented. The proposed model allows us to replace the 3D double corrugated cardboard by a 2D homogenized plate, which reduces a lot of time to calculate as well as time to build the geometry. Based on the theory of stratification and then improved by using the theory of sandwich, we calculated the rigidities of corrugated cardboard plate and then implemented into a 4-node shell element called S4R in Abaqus for an equivalent orthotropic plate. The results obtained by the present model are compared to those given by 3D shell simulations. The comparison shows the efficiency and accuracy of our homogenization model. The homogenization model can be used not only for corrugated cardboard plates, but also for industrial composite structures.

**Keywords**—Analytical homogenization, corrugated cardboard, orthotropic plates.

## I. INTRODUCTION

**S**ANDWICH structures have been used over a long time applications where the weight of the member is critical, such as packaging, civil, naval, automotive and aerospace industries due to their low mass to stiffness ratio and high impact absorption capacity [1]. Some instances of their applications in daily life are corrugated sandwich cores used for packaging, metal corrugated roofs, hulks, automotive chassis and bumpers. In nature, where mechanical design required to be optimized, sandwich structures are used such as the human skull, which is made up of two layers of dense compact bone separated by a “core” of lower density material.

A branch of sandwich structures is the corrugated cardboard panels consisting of three or more layers. The flat layers are called liners, which are partitioned by corrugated cores that are referred to as flutes. Paperboard structural material is a kind of environmental friendly packaging material made of reusable paper and water-based glue, which are 100% recyclable, reusable and fully biodegradable. So, it can settle the important strategic issue of the environment pressure, particular in relation to concerns over the amount of packaging waste, and has economic and environmental advantages over

plastic foams [2-3]. It belongs to a kind of inexpensive packaging material with corrugated sandwich structure, holds lightweight, high strength-to-weight and stiffness-to-weight ratios [4]. The corrugated core increases the moment of inertia of sandwich panel. Thus, the bending stiffness of corrugated panel has a direct relation with the third power of panel thickness. Although increasing the thickness of the sandwich panel by using a corrugated core with a low specific weight, results in a little increase in weight of panel, but this increases the strength of panel significantly [1]. The manufacturing process gives three characteristic directions (Fig. 1): the machine direction (MD), the cross direction (CD), and the thickness direction (ZD).

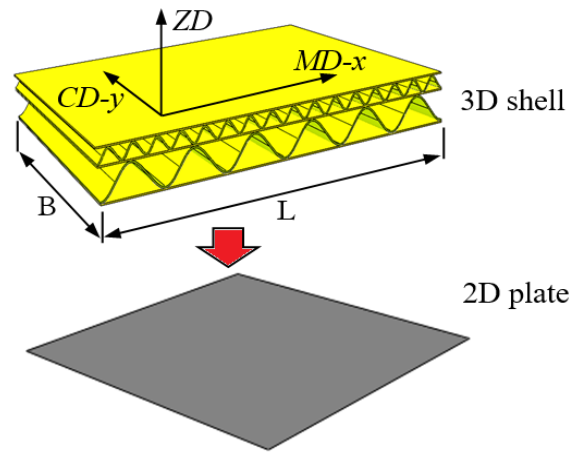


Fig. 1 Homogenization model

Corrugated cardboard is widely used in the packaging industry, such as corrugated cardboard boxes, insert cardboard sheet in pallet systems. It is essential to predict the mechanical behavior of these systems in order to use such materials effectively. The numerical modeling of this kind of orthotropic composite plates by shell elements is too tedious and time consuming. Many homogenization models were obtained by analytical, numerical and experimental methods [5-9]. By using some FE models and commercial FE software, the mechanical behaviors of corrugated cardboard were studied by other authors [10-13], but it just limited with the single corrugated cardboard.

This paper presents an efficient homogenization model for the mechanical behavior of a corrugated cardboard composed

of five layers (double flutes). The homogenization is carried out by calculating analytically the global rigidities of the corrugated cardboard and then this 3D structure is replaced by an equivalent homogenized 2D plate. The simulations under flexion and in-plane shear force of Abaqus-3D and H-2D model of double corrugated cardboard will be studied in this article. This 2D homogenization model is very fast and has close results comparing to the 3D model using the Abaqus shell elements.

II. RECALL OF MINDLIN’S THEORY AND THEORY OF LAMINATED PLATES

For a composite plate, the Mindlin theory is often used. It is assumed that a right segment and perpendicular to the mean surface remains straight but not perpendicular to the medium surface after deformation. This assumption allows to consider the transverse shear deformations. The membrane forces, bending moments and torsional and transverse shear forces are obtained by integration of the constraints on the thickness:

$$\{N(x, y)\} = \begin{Bmatrix} N_x \\ N_y \\ N_{xy} \end{Bmatrix} = \int_{-\frac{h}{2}}^{\frac{h}{2}} \begin{Bmatrix} \sigma_x \\ \sigma_y \\ \sigma_{xy} \end{Bmatrix} dz \tag{1}$$

$$\{M(x, y)\} = \begin{Bmatrix} M_x \\ M_y \\ M_{xy} \end{Bmatrix} = \int_{-\frac{h}{2}}^{\frac{h}{2}} z \begin{Bmatrix} \sigma_x \\ \sigma_y \\ \sigma_{xy} \end{Bmatrix} dz \tag{2}$$

$$\{T(x, y)\} = \begin{Bmatrix} T_x \\ T_y \end{Bmatrix} = \int_{-\frac{h}{2}}^{\frac{h}{2}} \begin{Bmatrix} \sigma_{xz} \\ \sigma_{yz} \end{Bmatrix} dz \tag{3}$$

If we consider a composite sheet consisting of several layers, the resulting forces defined above may be combined in layers:

$$\begin{Bmatrix} N_x \\ N_y \\ N_{xy} \end{Bmatrix} = \int_{-\frac{h}{2}}^{\frac{h}{2}} \begin{Bmatrix} \sigma_x \\ \sigma_y \\ \sigma_{xy} \end{Bmatrix} dz = \tag{4}$$

$$\sum_{k=1}^n \int_{h_{k-1}}^{h_k} \begin{bmatrix} Q_{11} & Q_{12} & 0 \\ Q_{12} & Q_{22} & 0 \\ 0 & 0 & Q_{33} \end{bmatrix}_k \left( \begin{Bmatrix} \varepsilon_x \\ \varepsilon_y \\ \varepsilon_{xy} \end{Bmatrix}_m + z \begin{Bmatrix} \kappa_x \\ \kappa_y \\ \kappa_{xy} \end{Bmatrix} \right) dz$$

$$\begin{Bmatrix} M_x \\ M_y \\ M_{xy} \end{Bmatrix} = \int_{-\frac{h}{2}}^{\frac{h}{2}} z \begin{Bmatrix} \sigma_x \\ \sigma_y \\ \sigma_{xy} \end{Bmatrix} dz = \tag{5}$$

$$\sum_{k=1}^n \int_{h_{k-1}}^{h_k} \begin{bmatrix} Q_{11} & Q_{12} & 0 \\ Q_{12} & Q_{22} & 0 \\ 0 & 0 & Q_{33} \end{bmatrix}_k \left( z \begin{Bmatrix} \varepsilon_x \\ \varepsilon_y \\ \varepsilon_{xy} \end{Bmatrix}_m + z^2 \begin{Bmatrix} \kappa_x \\ \kappa_y \\ \kappa_{xy} \end{Bmatrix} \right) dz$$

$$\begin{Bmatrix} T_x \\ T_y \end{Bmatrix} = \sum_{k=1}^n \int_{h_{k-1}}^{h_k} \begin{bmatrix} C_{11} & 0 \\ 0 & C_{22} \end{bmatrix}_k \begin{Bmatrix} \gamma_{xz} \\ \gamma_{yz} \end{Bmatrix} dz \tag{6}$$

After the integration along the thickness, we obtain the overall stiffness matrix that links the generalized deformations with resultant forces:

$$\begin{Bmatrix} N_x \\ N_y \\ N_{xy} \\ M_x \\ M_y \\ M_{xy} \\ T_x \\ T_y \end{Bmatrix} = \begin{bmatrix} A_{11} & A_{12} & 0 & B_{11} & B_{12} & 0 & 0 & 0 \\ A_{12} & A_{22} & 0 & B_{12} & B_{22} & 0 & 0 & 0 \\ 0 & 0 & A_{33} & 0 & 0 & B_{33} & 0 & 0 \\ B_{11} & B_{12} & 0 & D_{11} & D_{12} & 0 & 0 & 0 \\ B_{12} & B_{22} & 0 & D_{12} & D_{22} & 0 & 0 & 0 \\ 0 & 0 & B_{33} & 0 & 0 & D_{33} & 0 & 0 \\ 0 & 0 & 0 & 0 & 0 & 0 & F_{11} & 0 \\ 0 & 0 & 0 & 0 & 0 & 0 & 0 & F_{22} \end{bmatrix} \begin{Bmatrix} \varepsilon_{xm} \\ \varepsilon_{ym} \\ \gamma_{xym} \\ \kappa_x \\ \kappa_y \\ \kappa_{xy} \\ \gamma_{xz} \\ \gamma_{yz} \end{Bmatrix} \tag{7}$$

with

$$A_{ij} = \sum_{k=1}^n [h^k - h^{k-1}] Q_{ij}^k = \sum_{k=1}^n Q_{ij}^k t^k$$

$$B_{ij} = \frac{1}{2} \sum_{k=1}^n [(h^k)^2 - (h^{k-1})^2] Q_{ij}^k = \sum_{k=1}^n Q_{ij}^k t^k z^k$$

$$D_{ij} = \frac{1}{3} \sum_{k=1}^n [(h^k)^3 - (h^{k-1})^3] Q_{ij}^k \tag{8}$$

$$= \sum_{k=1}^n Q_{ij}^k \left[ t^k (z^k)^2 + \frac{(t^k)^3}{12} \right]$$

$$F_{ij} = \sum_{k=1}^n [h^k - h^{k-1}] C_{ij}^k = \sum_{k=1}^n C_{ij}^k t^k$$

The law of behavior above can be written in matrix form:

$$\begin{Bmatrix} \{N\} \\ \{M\} \\ \{T\} \end{Bmatrix} = \begin{bmatrix} [A] & [B] & [0] \\ [B] & [D] & [0] \\ [0] & [0] & [F] \end{bmatrix} \begin{Bmatrix} \{\varepsilon_m\} \\ \{\kappa\} \\ \{\gamma_s\} \end{Bmatrix} \tag{9}$$

where  $\{N\}$ ,  $\{T\}$  and  $\{M\}$  are the internal forces and moments;  $[A]$ ,  $[D]$ ,  $[B]$  and  $[F]$  are the stiffness matrices related to the membrane forces, the bending-torsion moments, the bending-torsion-membrane coupling effects and the transverse shear forces respectively;  $\{\varepsilon\}$  is the membrane strain vector,  $\{\kappa\}$  is the curvature vector and  $\{\gamma_s\}$  is the transverse shear strain vector.

III. HOMOGENIZATION MODEL FOR THE DOUBLE CORRUGATED CARDBOARD

A 3D geometrical modeling of the liners and the flutes of the corrugated cardboard is a very tedious and time-consuming task. In our homogenization model, a corrugated cardboard panel is replaced by a 2D plate. Instead of using a local constitutive law (relating the strains to the stresses) at each material point, the homogenization leads to global rigidities (relating the generalized strains to the resultant forces) for the equivalent homogeneous plate.

The corrugated cardboard is more complex than a laminated plate because of the fluting cores and the cavities between the

three liners. Consequently some global effective stiffnesses in the matrix (9) obtained by the theory of laminated plates should be modified [9, 12].

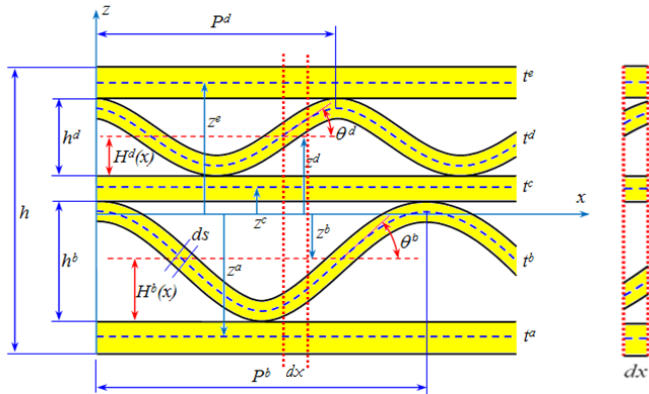


Fig. 2 Geometry of a double corrugated cardboard

Considering a double corrugated cardboard and using  $a$ ,  $b$ ,  $c$ ,  $d$ , and  $e$  to represent the lower liner, the lower flute, the intermediate liner, the upper flute and the upper liner (Fig. 2). The geometry of each flute is defined by the following equations:

$$\begin{cases} H^b(x) = \frac{h^b - t^b}{2} \sin\left(\frac{2\pi}{P^b}x\right) \\ \theta^b(x) = \tan^{-1}\left(\frac{dH^b(x)}{dx}\right) \\ H^d(x) = \frac{h^d - t^d}{2} \sin\left(\frac{2\pi}{P^d}x\right) \\ \theta^d(x) = \tan^{-1}\left(\frac{dH^d(x)}{dx}\right) \end{cases} \quad (10)$$

To homogenize a double corrugated panel, we consider a representative volume element (RVE). This volume must be sufficiently small relative to the dimensions of the entire panel. Once the overall stiffness of each slice are obtained by integrating the thickness, homogenization along  $x$  is performed to calculate the average stiffness of all tranches over a period:

$$\begin{aligned} [A] &= \frac{1}{P} \int_0^P [A(x)] dx; \quad [B] = \frac{1}{P} \int_0^P [B(x)] dx; \\ [D] &= \frac{1}{P} \int_0^P [D(x)] dx; \quad [F] = \frac{1}{P} \int_0^P [F(x)] dx \end{aligned} \quad (11)$$

We note that, in the Eq. 11, when periods  $P^d$  and  $P^b$  of corrugated layers are different, it is necessary to take an RVE having the length  $P$  that is the multiple of these periods.

### 3.1 Traction and bending stiffnesses related to $N_x$ , $M_x$ , $N_y$ , $M_y$

Since the vertical position ( $z$ ) of a groove portion ( $ds$ ) is a function of  $x$  and a thickness over its vertical section is a function of the angle of inclination of the groove  $\theta_x$  (Fig. 2),

the equation (8) becomes:

$$\begin{aligned} A_{ij} &= Q_{ij}^a t^a + Q_{ij}^b \frac{t^b}{\cos \theta^b} + Q_{ij}^c t^c + Q_{ij}^d \frac{t^d}{\cos \theta^d} + Q_{ij}^e t^e \\ B_{ij} &= Q_{ij}^a t^a z^a + Q_{ij}^b \frac{t^b}{\cos \theta^b} z^b + Q_{ij}^c t^c z^c + \\ &\quad + Q_{ij}^d \frac{t^d}{\cos \theta^d} z^d + Q_{ij}^e t^e z^e \\ D_{ij} &= Q_{ij}^a \left[ t^a (z^a)^2 + \frac{1}{12} (t^a)^3 \right] + \\ &\quad + Q_{ij}^b \left[ \frac{t^b}{\cos \theta^b} (z^b)^2 + \frac{1}{12} \left( \frac{t^b}{\cos \theta^b} \right)^3 \right] + \\ &\quad + Q_{ij}^c \left[ t^c (z^c)^2 + \frac{1}{12} (t^c)^3 \right] + \\ &\quad + Q_{ij}^d \left[ \frac{t^d}{\cos \theta^d} (z^d)^2 + \frac{1}{12} \left( \frac{t^d}{\cos \theta^d} \right)^3 \right] + \\ &\quad + Q_{ij}^e \left[ t^e (z^e)^2 + \frac{1}{12} (t^e)^3 \right] \end{aligned} \quad (12)$$

with

$$\begin{aligned} h &= t^a + h^b + t^c + h^d + t^e \\ z^a &= -\frac{h}{2} + \frac{t^a}{2}; \quad z^e = \frac{h}{2} - \frac{t^e}{2}; \quad z^c = -\frac{h}{2} + t^a + h^b + \frac{t^c}{2} \\ z^b(x) &= -\frac{h}{2} + t^a + \frac{h^b}{2} + \frac{1}{2} (h^b - t^b) \sin\left(\frac{2\pi}{P^b}x\right); \\ \frac{dz^b}{dx} &= \frac{\pi (h^b - t^b)}{P^b} \cos\left(\frac{2\pi}{P^b}x\right); \quad \theta^b(x) = \tan^{-1}\left(\frac{dz^b}{dx}\right) \\ z^d(x) &= \frac{h}{2} - t^e - \frac{h^d}{2} + \frac{1}{2} (h^d - t^d) \sin\left(\frac{2\pi}{P^d}x\right); \\ \frac{dz^d}{dx} &= \frac{\pi (h^d - t^d)}{P^d} \cos\left(\frac{2\pi}{P^d}x\right); \quad \theta^d(x) = \tan^{-1}\left(\frac{dz^d}{dx}\right) \end{aligned}$$

For each of the two grooves, a homogenization on their period (along  $x$ ) should be calculated numerically according to equation (11).

### 3.2 Shear stiffness in the $xy$ plane relative to $N_{xy}$ or $N_{yx}$

In a laminated composite plate, the integration through the thickness is used to calculate shear stiffness in the plane. This procedure consists in summing the product of the shear modulus and the thickness of all layers. However, it is no longer valid for corrugated cardboard because of the cavities.

Considering the corrugation of a corrugated board of length  $P/2$  (along  $x$ ) and width  $b$  (along  $y$ ) (Fig. 3). A pair of shear forces per unit of width  $N_{xy}$  (along  $y$ ) applied to the section MD gives a displacement  $v$ . The shearing of the groove can be easily treated by flattening the groove (Fig. 3b):

$$\tau_{12} = G_{12} \gamma_{12} \Rightarrow \frac{N_{xy}}{t} = G_{12} \frac{v}{0.5l} \quad (13)$$

where  $G_{12}$  is the shear modulus in the plane of the groove,  $l$  is the length of the flattened groove.

The shear deformation in the  $xy$  plane of the 3D groove (Fig. 3a) is defined by:

$$\gamma_{xy} = \frac{v}{0.5P} \tag{14}$$

Equations (13) and (14) make it possible to obtain the law of behavior for the shear in the  $xy$  plane:

$$N_{xy} = \frac{G_{12}Pt}{l} \gamma_{xy} \tag{15}$$

It can be shown that the average of the shear force on the CD section is equal to the shear force (constant) on the MD section. In fact, according to the reciprocity theorem, the flux of shear stress along the groove on CD is equal to that on MD ( $\tau_{yx} = \tau_{xy} = N_{xy}/t = const$ ); The component along  $x$  of this flux gives the shear force  $N_{yx}$ :

$$\begin{aligned} N_{yx} &= \frac{1}{0.5P} \int_0^{0.5P} \tau_{yx} t \cos \theta ds \\ &= \frac{1}{0.5P} \int_0^{0.5P} N_{xy} dx = N_{xy} \end{aligned} \tag{16}$$

So the relation  $N_{xy} = N_{yx}$  on MD and CD is proved and the shear stiffness is unique even if the two sections are very different.

For a double corrugated board, the shear stiffness in the plane of the cardboard is given by the sum of the rigidities of five layers:

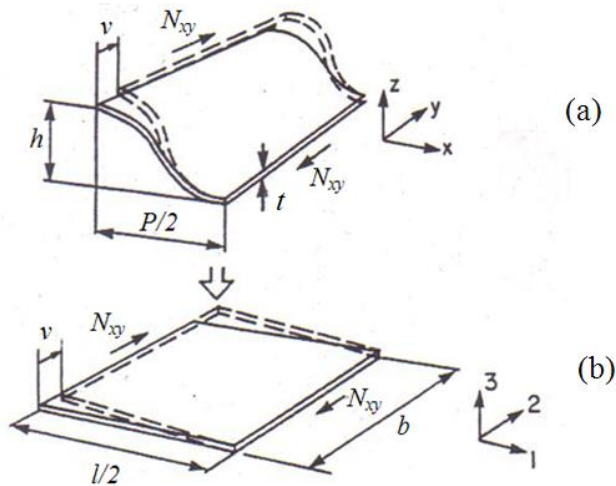


Fig. 3 Equivalent model for the shear of the groove in the  $xy$  plane

$$\begin{aligned} N_{xy} &= A_{33} \gamma_{xy}; \\ A_{33} &= G_{xy}^a t^a + \frac{G_{12}^b P^b t^b}{l^b} + G_{xy}^c t^c + \frac{G_{12}^d P^d t^d}{l^d} + G_{xy}^e t^e \end{aligned} \tag{17}$$

IV. RESULTS AND DISCUSSION

To validate our H-model, we first discretize the five layers of corrugated cardboard by shell elements S4R of Abaqus to obtain the model Abaqus-3D; Then, we discretize the middle surface of corrugated cardboard by shell elements S4R of Abaqus combined with our H-model (using "user's subroutine UGENS") to obtain H-2D model. The confrontation of the results allow us to evaluate the efficiency and accuracy of our homogenization model.

The calculations and comparisons are made on a double corrugated panel having CD section illustrated in Fig. 4. Geometric data are: period (or step) and height of the lower groove  $P^b = 9$  mm and  $h^b = 5.2$  mm, those of the upper groove  $P^d = 6$  mm and  $h^d = 2.9$  mm, thicknesses  $t^a = t^c = t^e = 0.25$  mm,  $t^b = t^d = 0.26$  mm. The properties of materials are given in Table 1 [9]. The rigidities of 2D equivalent plate are calculated as shown in Table 2.

We use a corrugated panel having length  $L = 162$  mm and width  $B = 180$  mm. This panel is tested under different types of loading: traction, bending and in-plane shear. For the simulation of the homogenized plate using our H-2D model, the middle surface is discretized into 7290 quadrilateral elements S4R and 7462 nodes. But for the Abaqus simulation-3D, 93825 quadrilateral elements S4R and 86925 nodes are needed. Indeed, to fully describe the geometry of the groove, it takes at least 16 elements over a period of groove.

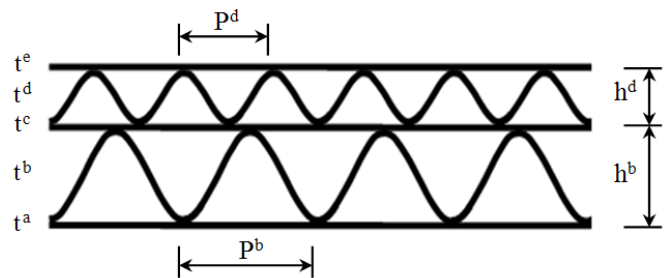


Fig. 4 Geometry of the CD section of corrugated cardboard

Table 1 Material properties of the five layers of the corrugated cardboard

| Layers | $E_1$<br>(MPa) | $E_2$<br>(MPa) | $E_3$<br>(MPa) | $G_{12}$<br>(MPa) | $G_{13}$<br>(MPa) | $G_{23}$<br>(MPa) | $\nu_{12}$ | $\nu_{13}$ | $\nu_{23}$ |
|--------|----------------|----------------|----------------|-------------------|-------------------|-------------------|------------|------------|------------|
| a      | 8250           | 2900           | 2900           | 1890              | 7                 | 70                | 0.43       | 0.01       | 0.01       |
| b, d   | 4500           | 4500           | 3000           | 1500              | 3.5               | 35                | 0.40       | 0.01       | 0.01       |
| c, e   | 8180           | 3120           | 3120           | 1950              | 7                 | 70                | 0.43       | 0.01       | 0.01       |

Table 2 Rigidities of the equivalent plate

| Rigidities | $A_{11}$<br>(N/mm) | $A_{12}$<br>(N/mm) | $A_{22}$<br>(N/mm) | $A_{33}$<br>(N/mm) | $B_{11}$<br>(N) | $B_{12}$<br>(N) | $B_{22}$<br>(N) | $D_{11}$<br>(N.mm) | $D_{12}$<br>(N.mm) | $D_{22}$<br>(N.mm) |
|------------|--------------------|--------------------|--------------------|--------------------|-----------------|-----------------|-----------------|--------------------|--------------------|--------------------|
| Values     | 6606.2             | 1055.1             | 5989.8             | 1964.9             | 2507.1          | 526.1           | 2914.5          | 75214.1            | 11870.5            | 49672.4            |

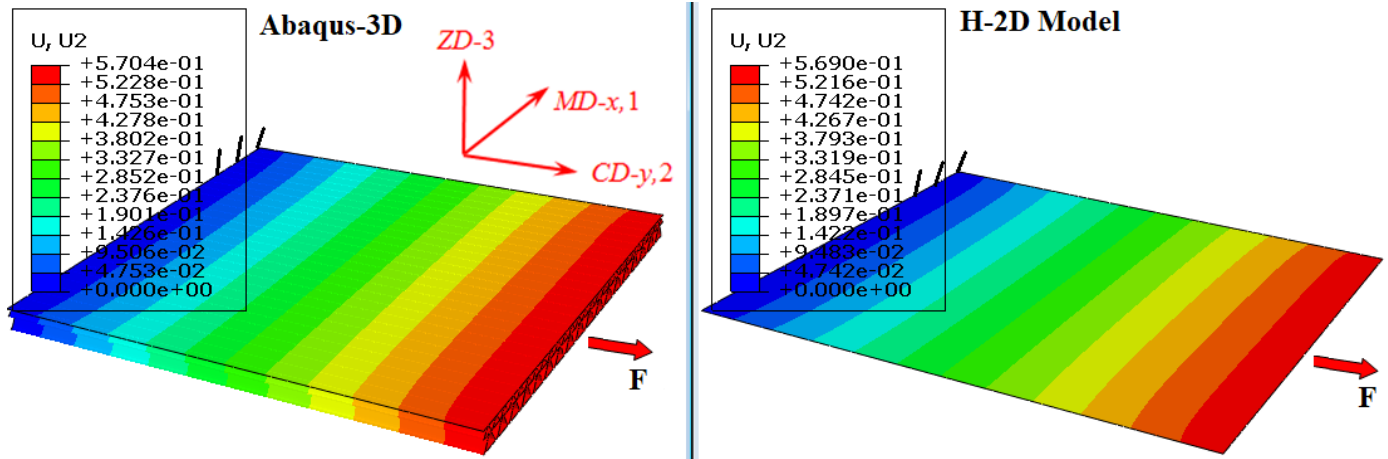


Fig. 5 Simulation of Abaqus-3D and H-model in traction for the CD section

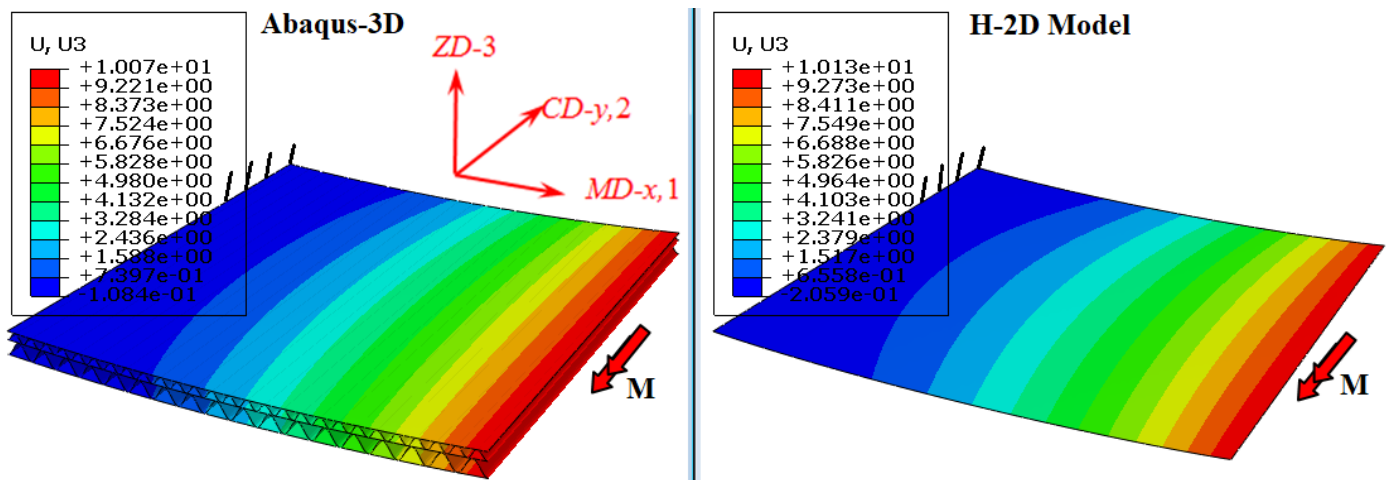


Fig. 6 Simulation of Abaqus-3D and H-model in bending for the MD section

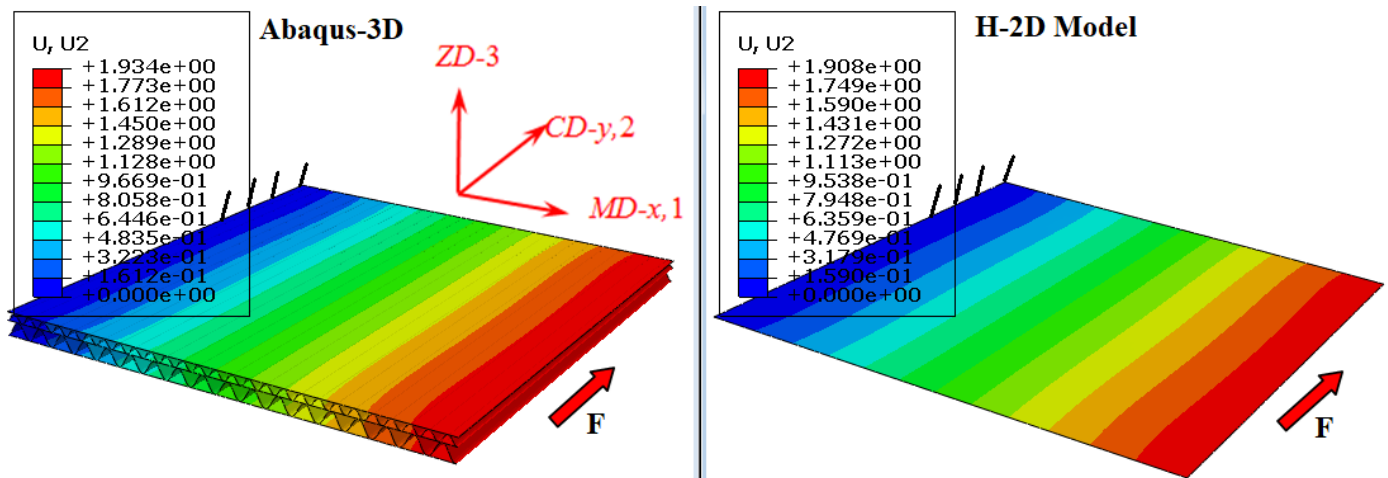


Fig. 7 Simulation of Abaqus-3D and H-model in in-plane shear for the MD section

Table 3 Comparison between Abaqus-3D and H-2D-Model for the plate under traction, flexion and in-plane shear loading

|                             |    |                         | Abaqus-3D | H-2D-Model | Error (%)   |
|-----------------------------|----|-------------------------|-----------|------------|-------------|
| Traction<br>$F=3000N$       | MD | Displacement $U_1$ (mm) | 0.4304    | 0.4270     | -0.79       |
|                             |    | CPU time (s)            | 70.2      | 1.6        | 43.9 times  |
|                             | CD | Displacement $U_2$ (mm) | 0.5704    | 0.5690     | -0.24       |
|                             |    | CPU time (s)            | 65.6      | 1.5        | 43.7 times  |
| In-plane shear<br>$F=3000N$ | MD | Displacement $U_2$ (mm) | 1.934     | 1.908      | -1.34       |
|                             |    | CPU time (s)            | 59        | 1.4        | 42.14 times |
|                             | CD | Displacement $U_1$ (mm) | 2.684     | 2.656      | -1.04       |
|                             |    | CPU time (s)            | 63        | 1.4        | 45 times    |
| Bending<br>$M=10 KN.mm$     | MD | Displacement $U_3$ (mm) | 21.43     | 21.53      | +0.47       |
|                             |    | CPU time (s)            | 58.2      | 1.6        | 36.38 times |
|                             | CD | Displacement $U_3$ (mm) | 10.07     | 10.13      | +0.59       |
|                             |    | CPU time (s)            | 57.5      | 1.5        | 38.33 times |

In both types of simulations (Abaqus-3D model and H-2D model), a rigid plate is bonded to the MD or CD section at the right end of the cardboard panel to better apply forces or moments (Fig. 5, 6, 7). The calculations by our H-2D model are very fast while calculations by Abaqus-3D are much longer. The comparisons of results obtained by the two models and the percentages of error in H-2D model compared to Abaqus-3D results for the traction, bending and in-plane shear loading are presented in Table 3, we note that the numerical results given by the two models are very close.

## V. CONCLUSION

In this article, we have proposed an analytic homogenization model for the traction, flexion and in-plane shear problems of double corrugated core cardboards. The comparison of the results obtained by the analytic formulas, by the Abaqus 3D simulations and by the Abaqus-Ugens 2D simulations has proved the validation of the present homogenization model in the case of traction, flexion and in-plane shear loading. The present H-model allows us to largely reduce not only the time for the geometry creation and FE calculation, but also the computational hardware requirements for the large-scale numerical modelling of packaging systems composed of double corrugated core cardboards.

## REFERENCES

- [1] Iman Dayyani, Saeed Ziaei-Rad and Michael I Friswell, The mechanical behavior of composite corrugated core coated with elastomer for morphing skins, *Journal of Composite Materials*, 48, 1623–1636, 2014.
- [2] Kirkpatrick J, Sek M. Replacement of polymeric cushioning with corrugated fiberboard-case study. *Proceedings of 10th IAPRI World Conference on Packaging*, Australia, Melbourne, 267-276, 1997.
- [3] Coles R, Mcdowell D, Kirwan M J. Food packaging technology. *CRC Press*, 2003

- [4] Kooistra G W, Deshpande V, Wadley H N G. Hierarchical corrugated core sandwich panel concepts. *Journal of Applied Mechanics*, 74(1): 259-268, 2007.
- [5] Carlsson L.A., Nordstrand T., Westerlind B., On the elastic stiffness of corrugated core sandwich plate, *J Sandwich Structures and Materials*, 3, 253–267, 2001.
- [6] Aboura Z., Talbi N., Allaoui S., Benzeggagh M.L., Elastic behaviour of corrugated cardboard: experiments and modeling, *Composite Structures*, 63, 53–62, 2004.
- [7] Buannic N., Cartraud P., Quesnel T., Homogenization of corrugated core sandwich panels, *Composite Structures*, 59, 299–312, 2003.
- [8] Biancolini M.E. Evaluation of equivalent stiffness properties of corrugated board, *Composite Structures*, 69, 322–328, 2005.
- [9] Talbi N., Batti A., Ayad R., Guo Y.Q., An analytical homogenization model for finite element modelling of corrugated cardboard, *Composite Structures*, 69, 322–328, 2005.
- [10] Biancolini M.E., Brutti C., Numerical and Experimental Investigation of the Strength of Corrugated Board Packages, *Packaging Technology and Science*, 16, 47–60, 2003.
- [11] Rami H.A., Choi J., Wei B.S., Popil R., Schaepe M., Refined Nonlinear Finite Element Models for Corrugated Fiberboards, *Composite Structures*, 87, 321–333, 2009.
- [12] Abbès B., Guo Y.Q., Analytic homogenization for torsion of orthotropic sandwich plates: application to corrugated cardboard, *Composite Structures*, 92, 699–706, 2010.
- [13] Nordstrand T., On buckling loads for edge-loaded orthotropic plates including transverse shear. *Composite Structures* 65, 1–6, 2004.